symmetry

MDPI

Article

Electromagnetic Fields around Black Holes in Einstein Æther Gravity

Javlon Rayimbaev [1,2,3,4,5], Bobomurat Ahmedov [1,4,5,6,*] and Eldor Karimbaev [5,7]

1 Ulugh Beg Astronomical Institute, Astronomy St. 33, Tashkent 100052, Uzbekistan
2 College of Engineering, Akfa University, Kichik Halqa Yuli Street 17, Tashkent 100095, Uzbekistan
3 Power Engineering Faculty, Tashkent State Technical University, Tashkent 100095, Uzbekistan
4 Faculty of Physics, National University of Uzbekistan, Tashkent 100174, Uzbekistan
5 Institute of Fundamental and Applied Research, National Research University TIIAME, Kori Niyoziy 39, Tashkent 100000, Uzbekistan
6 Tashkent Institute of Irrigation and Agricultural Mechanization Engineers, Kori Niyoziy, 39, Tashkent 100000, Uzbekistan
7 Institute of Nuclear Physics, Ulugbek 1, Tashkent 100214, Uzbekistan
* Correspondence: ahmedov@astrin.uz

Abstract: Axial symmetry and stationary properties of spacetime allow to find exact analytical solutions of differential equations describing fields and particles in a gravitational background. The present work is mainly devoted to derivation of exact solutions of Maxwell's equations for magnetic fields generated by current loops around static black holes (BHs) in Einstein-aether gravity based on the spacetime symmetries in both regions: (i) interior and (ii) exterior to the current loop for a proper observer. The spacetime symmetries are applied in separating variables to solve the second order ordinary differential equation for vector potential of electromagnetic field and the equations of motion of test particles around the aether BH. We also study effects of the aether field on innermost stable circular orbits (ISCOs) of the test particles assuming the current loop position is placed there. It is obtained that the ISCO radius, as well as dipole magnetic moment of the current loop decrease with the increase of the aether parameter c_{14}. Moreover, the performed analysis indicates that the aether field causes a decrease in the magnetic field inside and outside the current loop due to the change of its position.

Keywords: black holes; magnetic fields; symmetries in gravity; Einstein aether theory

PACS: 04.50.-h; 04.40. Dg; 97.60. Gb

Citation: Rayimbaev, J.; Ahmedov, B.; Karimbaev, E. Electromagnetic Fields around Black Holes in Einstein Æther Gravity. *Symmetry* **2022**, *14*, 1809. https://doi.org/10.3390/sym14091809

Academic Editor: Kazuharu Bamba

Received: 31 July 2022
Accepted: 27 August 2022
Published: 1 September 2022

1. Introduction

General Relativity (GR) is a classical theory of gravity which was proposed by Einstein in 1915, and was successfully tested for the first time in 1919 using solar eclipse in the weak gravitational field and slow motion regime. However, 100 years later, there is still no properly constructed and developed quantum gravity theory. The physical vacuum in quantum gravity may determine a preferred rest frame at the microscopic level. Numerous observations severely limit the possibility of Lorentz-violating physics among the standard model gravitational fields. The constraints on Lorentz violation in the gravitational sector are generally far weaker.

To allow for gravitational Lorentz violation without abandoning the framework of GR, the background tensor fields breaking the symmetry are requested to have dynamical behaviour. Einstein-aether gravity theory is also one of this type of field theories [1]. In addition to the spacetime metric tensor, it involves a dynamical, unit timelike vector field. Like the metric, and unlike other classical fields, the unit vector cannot vanish anywhere, so it breaks local Lorentz symmetry down to a rotation subgroup. It defines a congruence

of timelike curves filling the whole spacetime, similar to a fluid, and so it has been referred to as an "aether".

The motivation for studying the Einstein-aether gravity theory is manyfold. The first primary goal is related to the quantum gravity suspicion already discussed. A secondary goal is to develop a viable and reasonably natural foil against which to constrain theories of gravity through the current gravitational and astronomical observations, in an era of great discoveries in relativistic astrophysics when numerous alternative gravity theories have already been either ruled out or severely constrained. The third goal of interest in the Einstein-aether gravity theory is the theoretical laboratory it offers for studying symmetries and diffeomorphism-invariant physics with preferred frame effects.

Geometrically, the Einstein-aether gravity theory is a vector-tensor gravity theory where the vector field is constrained to have a unit norm. These constraints eliminate a wrong-sign kinetic term for the length-stretching mode, providing the tested theory with a possibility of being viable [2].

From the basic principles, general relativity is based on an inertial frame of reference only on the local scale. Indeed, it can not behave in this way as a global inertial frame. On the other hand, a gravitating body is considered as immersed in an aether field in the framework of the Einstein-aether gravity theory. Accordingly, a timelike direction at a given point of spacetime with Lorentz symmetry can be defined in the Einstein-aether gravity while it is violated in general relativity [3]. Astrophysical and cosmological aspects of the Einstein-aether gravity are explored in [4,5]. The paper [6] is devoted to thermodynamics of the Einstein-aether gravity. Dynamics and motion of test particles in close vicinity of BHs in the aether gravity are investigated in [7,8]. The constraints on the parameters of the Einstein-aether gravity are obtained through LIGO-VIRGO gravitational waves observations [9,10]. The first image of the supermassive black hole (SMBH) M 87* by the Event Horizon Telescope (EHT) also provided observational constraints on the Einstein-aether gravity parameters [11].

The main properties (including the critical mass limit) of the relativistic neutron stars in the Einstein-aether gravity are probed in Refs. [1,12]. Using numerical studies of the equations of state for a relativistic star assuming its inner matter as a perfect fluid are performed in Ref. [13], and it is shown that the existence of an exterior, static aether field can be also a cause of the stability in the density of the stars.

According to the well-known no-hair theorem, BHs do not have their own intrinsic magnetic fields. However, there are two astrophysical scenarios when the magnetic fields can exist around BHs: (i) an external magnetic field generated by the companion gravitational object (e.g., binary systems of a BH and neutron star), (ii) an electromagnetic field can be produced by the charged particles orbiting the BHs which can be modelled as a current loop.

The exact analytical solutions of the general relativistic Maxwell equations for the magnetic field of the gravitating object has been pioneered by Ginzburg and Ozernoi in 1964. Wald in 1974 [14] assumed a Schwarzschild BH is embedded in an asymptotically uniform magnetic field and presented the exact analytical solution for the electromagnetic field. Petterson in Ref. [15] presented exact solution for the dipolar electromagnetic field produced by the electric current loop around the Schwarzschild BH. Later, the related problems of the electrodynamics in the curved spacetime are extended to the alternative theories of gravity [16,17].

The electromagnetic fields of a magnetized sphere, which has a dipole magnetic moment, have been studied in Ref. [18]. Electrodynamics of the relativistic magnetised neutron stars is explored in the frame of various gravity theories, including GR in [19–24].

Estimations of magnetic field strength around stellar and supermassive BHs have shown that their values can be maximum in the order of $\sim 10^8$ G near stellar BHs and $\sim 10^4$ G in the vicinity of SMBHs (see, for example, [25]). Observational data of the SMBH M87* show that magnetic field strength around the BH is around $B \sim$1–30 G [26]. The

magnetic field near the SMBH Sgr A*, determined by the dispersion measure of the plasma medium around it, is a few milli Gs [27].

We organize the paper as follows: Section 2 is devoted to the analysis of a BH solution in Einstein-aether gravity. The circular motion of test particles around the aether BH is studied in Section 3. Exact analytical solutions for multipolar magnetic fields generated by the current loop around an aether BH are obtained in Section 4 where a detailed analysis of the aether field effects on the magnetic fields is provided. The main results are summarized in Section 5.

Throughout this work, we use the space-like signature $(-, +, +, +)$ and geometrized units of the system where $G = 1 = c$. Moreover, we let run the Latin (Greek) indices from 1 (0) to 3.

2. Black Holes in Einstein-Aether Gravity

It is requested to add to the well-known Einstein–Hilbert action an Einstein-aether gravity term, being responsible for a dynamical and unit timelike aether field [1,3,28,29]. The action of Einstein-aether theory cannot vanish anywhere, breaking Lorentz symmetry locally. The complete form of its action has the following form,

$$S = \frac{1}{16\pi G}\int d^4x\sqrt{-g}(R + \mathcal{L}_{ae})\,, \tag{1}$$

where $g = |g_{\mu\nu}|$ is the determinant of the spacetime metric around the BH in the aether gravity. The Lagrangian density for the aether field reads as,

$$\mathcal{L}_{ae} = -M^{\alpha\beta}{}_{\mu\nu}(D_\alpha u^\mu)(D_\beta u^\nu) + \lambda(g_{\mu\nu}u^\mu u^\nu + 1)\,, \tag{2}$$

where λ is the Lagrangian multiplier which is responsible for the Æther four-velocity u^α always to be timelike, D_α is the covariant derivative with respect to the coordinate x^α, and $M^{\alpha\beta}{}_{\mu\nu}$ is defined as

$$M^{\alpha\beta}{}_{\mu\nu} = c_1 g_{\mu\nu}g^{\alpha\beta} + c_2\delta^\alpha_\mu\delta^\beta_\nu + c_3\delta^\alpha_\nu\delta^\beta_\mu - c_4 u^\alpha u^\beta g_{\mu\nu}, \tag{3}$$

where c_i $(i = 1, 2, 3, 4)$ are gravitational coupling constants of the aether field being dimensionless. The gravitational constant in the aether field theory can be described by the gravitational constant in Newtonian gravity G_N in the following form,

$$G = \frac{G_N}{1 - \frac{1}{2}c_{14}}\,, \tag{4}$$

where $c_{14} = c_1 + c_4$, is a new coupling parameter of the aether field.

The special class BH solution of the field equation within the Einstein-aether theory (1) has the line element in the spherical coordinates [30]:

$$ds^2 = -f(r)dt^2 + \frac{dr^2}{f(r)} + r^2(d\theta^2 + \sin^2\theta d\phi^2)\,, \tag{5}$$

where

$$f(r) = 1 - \frac{2M}{r} + \frac{2c_{13} - c_{14}}{2(1 - c_{13})}\frac{M^2}{r^2}\,, \tag{6}$$

with the new coupling constant $c_{13} = c_1 + c_3$ and. it is $c_{13} \neq 1$. In two different cases, the metric (5) reflects properties of static metric, Schwarzschild BH spacetime metric, when, (i) $c_{13} = c_{14} = 0$ and (ii) $2c_{13} = c_{14}$. Moreover, one can see from Equation (4)

Figure 1 shows the dependence of the radius of outer horizon of an aether BH from the aether field parameter c_{14}, for the different values of c_{13}. It is observed from the figure that an increase of c_{14} causes the decrease in the radius.

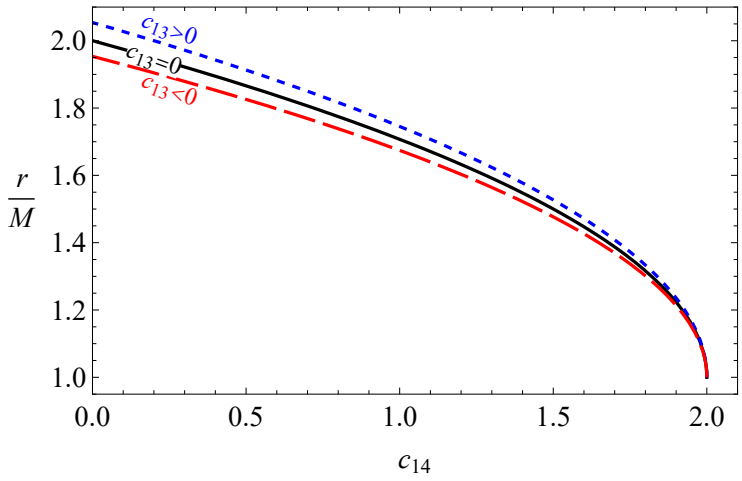

Figure 1. Radius of outer horizon of static BHs in Einstein Aether BHs.

3. Dynamics of Test Particles around Aether BHs

Now, we investigate the dynamics of electrically neutral test particles around an aether BH, paying our attention to considering only circular stable orbits.

The Lagrangian for test particles with rest mass m, orbiting a BH reads as

$$L_{\rm p} = \frac{1}{2} m g_{\mu\nu} \dot{x}^\mu \dot{x}^\nu. \tag{7}$$

It is difficult to find analytical solutions of the equations of motion unless integrals of motion are introduced. Fortunately, in axial symmetric and stationary spacetime, it is possible to introduce the Killing vectors generated by the symmetry of the spacetime which is responsible for the conservation of energy and angular momentum of the particle along the geodesic motion.

The corresponding conserved quantities can be calculated using the Killing vectors

$$\xi^\mu_{(t)} \partial_\mu = \partial_t, \qquad \xi^\mu_{(\phi)} \partial_\mu = \partial_\phi, \tag{8}$$

where $\xi^\mu_{(t)} = (1,\ 0,\ 0,\ 0)$ and $\xi^\mu_{(\phi)} = (0,\ 0,\ 0,\ 1)$, which are corresponding to the energy and angular momentum of the particles $\mathcal{E} = E/m$ and $\mathcal{L} = L/m$, respectively, with equations,

$$\dot{t} = \frac{\mathcal{E}}{g_{tt}}, \quad \dot{\phi} = \frac{\mathcal{L}}{g_{\phi\phi}}. \tag{9}$$

Here, we derive the equations of motion using the following normalization condition,

$$g_{\mu\nu} u^\mu u^\nu = -1. \tag{10}$$

Equations of motion for test particles which are around a static BH take the following form using Equations (9) and (10),

$$\dot{r}^2 = \mathcal{E}^2 + g_{tt}\left(1 + \frac{\mathcal{K}}{r^2}\right), \tag{11}$$

$$\dot{\theta}^2 = \frac{1}{g^2_{\theta\theta}}\left(\mathcal{K} - \frac{\mathcal{L}^2}{\sin^2\theta}\right), \tag{12}$$

with the Carter constant $\mathcal{K}$.

In this work, we investigate the particle's motion in the constant plane $p_\theta = 0$. At the equatorial plane, the constant $\mathcal{K}$ will be $\mathcal{K} = \mathcal{L}^2$ and one can obtain,

$$\dot{r}^2 = \mathcal{E}^2 - V_{\rm eff} \tag{13}$$

where $V_{\rm eff}$ is the effective potential, and it has the following form,

$$V_{\rm eff} = f(r)\left(1 + \frac{\mathcal{L}^2}{r^2 \sin^2\theta}\right). \tag{14}$$

To study the circular motion of the test particle, consequently, we consider the conditions that imply there are no radial motions ($\dot{r} = 0$) and no forces in the radial direction ($\ddot{r} = 0$) [31,32]. Using this condition, one can obtain expressions for the specific angular momentum and a specific energy for circular orbits in the equatorial plane ($\theta = \pi/2$) where the effective potential as given in Equation (14) is maximal

$$\mathcal{L}^2(r) = \frac{Mr^2(\alpha M + r)}{-2\alpha M^2 - 3Mr + r^2}, \qquad \mathcal{E}^2(r) = \frac{\left(\alpha M^2 + 2Mr - r^2\right)^2}{r^2(-2\alpha M^2 - 3Mr + r^2)}, \tag{15}$$

where

$$\alpha = \frac{2c_{13} - c_{14}}{2(1 - c_{13})}$$

is a new constant.

ISCOs around an Aether BH

Basically, the stability of a test particle's circular orbits in axially symmetric spacetime defines the condition $V''_{\rm eff} \geq 0$, and ISCO radius is found as a solution of the equation $\partial_{rr} V_{\rm eff} = 0$, and in our case i.e., in the equatorial plane around the Einstein aether BH, we have,

$$\begin{aligned} r_{ISCO} &= \frac{1}{2}\left(1 - i\sqrt{3}\right)\sqrt[3]{\alpha\sqrt{\alpha+1}\sqrt{4\alpha+5}M^3 - (\alpha(2\alpha+9)+8)M^3} \\ &+ \frac{\left(1 + i\sqrt{3}\right)(3\alpha+4)M^2}{2\sqrt[3]{\alpha\sqrt{\alpha+1}\sqrt{4\alpha+5}M^3 - (\alpha(2\alpha+9)+8)M^3}} + 2M \end{aligned} \tag{16}$$

The relationships between the ISCO radius for test particles around the aether BH and the aether field parameters c_{14} are presented in Figure 2, for positive and negative values of c_{13}. It is obtained that the ISCO radii increase (decrease) when the parameter c_{13} is positive (negative) at values of the parameter c_{14} near zero. Furthermore, as c_{14} approaches 2, the effects of c_{13} on the ISCO radius vanish, and at $c_{14} = 2$ the radius takes the value $r_{ISCO} = 4M$.

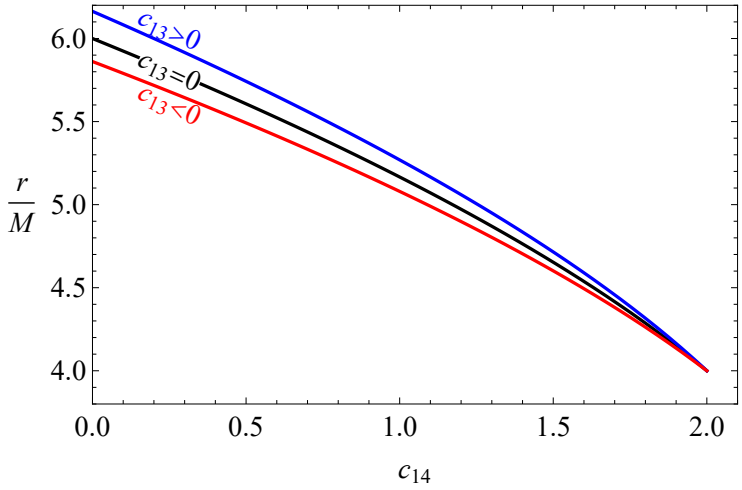

Figure 2. Dependence of the ISCO radius of test particles around the aether BHs from the aether parameter c_{14}, for the different values of c_{13}.

4. Magnetic Field Solutions of Maxwell Equations in Spacetime around BHs in Einstein-Aether Gravity

In the present section, we plan to find the solution of the Maxwell equations for the magnetic field of the current loop around static BHs in the aether theory. Petterson was the first to consider the problem in Schwarzschild spacetime in Ref. [15].

Maxwell's equations in the curved spacetime take the form

$$\partial_\mu(\sqrt{-g}F^{\mu\nu}) = 4\pi\sqrt{-g}J^\nu, \quad \partial_\mu(\sqrt{-g}\,{}_*F^{\mu\nu}) = 0 \tag{17}$$

where $F^{\mu\nu}$ is the electromagnetic field tensor and its dual one is ${}_*F^{\mu\nu} = \frac{1}{2!}\epsilon^{\mu\nu\gamma\rho}F_{\gamma\rho}$, the tensor $\eta_{\alpha\beta\sigma\gamma}$ is expressed through the antisymmetric symbol of Levi-Civita $\epsilon_{\alpha\beta\sigma\gamma}$ as

$$\eta_{\alpha\beta\sigma\gamma} = \sqrt{-g}\epsilon_{\alpha\beta\sigma\gamma}\,, \qquad \eta^{\alpha\beta\sigma\gamma} = -\frac{1}{\sqrt{-g}}\epsilon^{\alpha\beta\sigma\gamma}\,, \tag{18}$$

and the determinant of the metric tensor (5) is $g = -r^4\sin^2\theta$, J^μ is a four-current vector as a source of the magnetic field around the BH. Here, is assumed that the loop carrying an electric current is placed at an equatorial plane near ISCO ($r_0 = r_{ISCO}$), and the electric current has only an azimuthal component ($J^t = J^r = J^\theta$=0):

$$J^\phi = \frac{I}{r^2}\sqrt{f(r)}\delta(r-r_0)\delta(\cos\theta)\,. \tag{19}$$

Finding analytical solutions to the Maxwell equations requires the symmetry of the spacetime metric. In order to separate variables in the differential equation. For example, R. Wald in his pioneering study of BH electrodynamics, obtained the exact solutions of Maxwell equations using the time-like and space-like Killing vectors responsible for the axial symmetry of the spacetime.

Since the current loop is at the equatorial plane, due to axial symmetric behavior of the spacetime, one may consider that the vector potential depends on only r and θ coordinates ($A_\phi(r,\theta)$). The Maxwell equation for the axial symmetry and stationary electromagnetic fields in Equation (17) takes the following form in the spacetime (5),

$$\begin{aligned}\frac{1}{\sin\theta}\frac{\partial}{\partial r}\Big(f(r)\frac{\partial}{\partial r}A_\phi(r,\theta)\Big) &+ \frac{1}{r^2\sin\theta}\frac{\partial}{\partial\theta}\Big(\frac{1}{\sin\theta}\frac{\partial}{\partial\theta}A_\phi(r,\theta)\Big)\\ &= -4\pi I\sqrt{f(r)}\delta(r-r_0)\delta(\cos\theta)\,.\end{aligned} \tag{20}$$

Here, we look for the solution of Equation (20) as a separable form,

$$A_\phi(r,\theta) = \mathcal{R}(r)\Theta(\theta)\,, \tag{21}$$

and we can immediately get the following two independent equations:

$$\sin\theta\frac{d}{d\theta}\Big(\frac{1}{\sin\theta}\frac{d\Theta_l(\theta)}{d\theta}\Big) + (l+1)(l+2)\Theta_l(\theta) = 0\,, \tag{22}$$

$$r^2\frac{d}{dr}\Big(f(r)\frac{d\mathcal{R}_l(r)}{dr}\Big) - (l+1)(l+2)\mathcal{R}_l(r) = 0\,, \tag{23}$$

where l is a multipole number which can only be an integer. It is quite a long way to solve Equations (22) and (23) for arbitrary numbers of l. For simplicity, we find the solutions of the equations for the case of $l = 0$. From this point, we call $\mathcal{R}_0(r)$ as $\mathcal{R}(r)$ and $\Theta_0(\theta)$ as $\Theta(\theta)$, and in this case the regular solution of Equation (23) is $\Theta(\theta) = \sin^2\theta$, so we have a simplified equation for the radial function as,

$$\Big[(r-M)^2 - M^2(1-\alpha)\Big]\mathcal{R}''(r) + 2M\Big(1+\alpha\frac{M}{r}\Big)\mathcal{R}'(r) - 2\mathcal{R}(r) = 0\,. \tag{24}$$

Now, an exact solution of Equation (22) can be obtained in the form,

$$\mathcal{R}(r) = a_1\mathcal{R}_1(r) + a_2\mathcal{R}_2(r)\,, \tag{25}$$

where,

$$\mathcal{R}_1(r) = r^2 + \alpha M^2\,, \tag{26}$$

$$\mathcal{R}_2(r) = \frac{1}{8(1+\alpha)^{\frac{3}{2}}M^3}\Big[2M(r+M)\sqrt{1+\alpha} + (r^2+\alpha M^2)\ln\Big(1 - \frac{2M\sqrt{1+\alpha}}{r - M(1-\sqrt{1+\alpha})}\Big)\Big]\,. \tag{27}$$

Thus, we have obtained an expression for A_ϕ, in the following form,

$$A_\phi(r,\theta) = (a_1\mathcal{R}_1(r) + a_2\mathcal{R}_2(r))\sin^2\theta\,. \tag{28}$$

Now, we aim to find the regular solution for the electromagnetic four-potential (28) in the interior of the current loop, as well as exterior regions. In the interior region where $2M \leq r \leq r_0$, only $\mathcal{R}_1(r)$ function can be a solution, due to non-regularity of the function $\mathcal{R}_2(r)$ at the horizon $r = r_h$, it implies that the constant $a_2 = 0$.

For $r > r_0$ regions, $\mathcal{R}_1(r)$ may be the solution for A_ϕ, when $a_1 = 0$, due to non-regularity of $\mathcal{R}_2(r)$ at $r \to \infty$. Thus, we use the boundary condition for the potential to be continuous at $r = r_0$, so A_ϕ takes the following form,

$$A_\phi(r,\theta) = a_1\mathcal{F}(r)\sin^2\theta\,, \tag{29}$$

where,

$$\mathcal{F}(r) = \begin{cases} \mathcal{R}_1(r)\mathcal{R}_2(r_0), & r_+ \leq r \leq r_0\,, \\ \mathcal{R}_1(r_0)\mathcal{R}_2(r), & r \geq r_0\,. \end{cases} \tag{30}$$

Now, we get a new differential equation for $\mathcal{F}(r)$ by inserting Equation (29) into the Maxwell's Equation (20) in the following form,

$$a_1\sin\theta\Big[\frac{d}{dr}\Big(f(r)\frac{d\mathcal{F}(r)}{dr}\Big) - \frac{2\mathcal{F}(r)}{r^2}\Big] = -4\pi I\sin\theta\sqrt{f(r)}\delta(r-r_0)\delta(\cos\theta)\,. \tag{31}$$

First, one can multiply left hand and right hand sides of Equation (31) with term $\sin\theta$, then integrate it over $\cos\theta$, and get,

$$a_1\Big[\frac{d}{dr}\Big(f(r)\frac{d\mathcal{F}(r)}{dr}\Big) - \frac{2\mathcal{F}(r)}{r^2}\Big] = -4\pi I\sqrt{f(r)}\delta(r-r_0)\,. \tag{32}$$

From the solution of Equation (32) at ISCO ($r = r_0$), considering the current loop is an infinitesimal thin disk, we get,

$$a_1\sqrt{f(r)}\mathcal{F}'(r_0) = -3\pi I\,, \tag{33}$$

where $'$ denotes the derivative with respect to r, and $\mathcal{F}'(r_0)$ is the value of the first derivative of the function $\mathcal{F}(r)$ at $r = r_0$.

It is easy to find using Equations (30) and (32) the following relation,

$$\mathcal{F}'(r_0) = \frac{1}{f(r_0)}\,. \tag{34}$$

One may find the unknown integral constant using Equations (33) and (34) as,

$$a_1 = -3\pi I\sqrt{f(r)}\,. \tag{35}$$

Taking into account, Equations (31) and (35), we may have the following exact solution of the Maxwell equation with respect to the azimuthal component of the electromagnetic vector potential,

$$\begin{aligned} A_\phi &= -\frac{3\mu\sin^2\theta}{8(1+\alpha)^{\frac{3}{2}}M^3}(r^2+\alpha M^2) \\ &\times \begin{cases} \frac{2\sqrt{1+\alpha}M(r_0+2M)}{r_0^2+\alpha M^2} + \ln\left(1-\frac{2M\sqrt{1+\alpha}}{r_0-M(1-\sqrt{1+\alpha})}\right), & r_+ \le r \le r_0\,, \\ \frac{2\sqrt{1+\alpha}M(r+2M)}{r^2+\alpha M^2} + \ln\left(1-\frac{2M\sqrt{1+\alpha}}{r-M(1-\sqrt{1+\alpha})}\right), & r \ge r_0\,, \end{cases} \end{aligned} \tag{36}$$

where the current loop around the aether BH is responsible for the magnetic moment μ:

$$\mu = \pi r_0^2\sqrt{f(r_0)}I\left(1+\alpha\frac{M^2}{r_0^2}\right). \tag{37}$$

In Figure 3 we test the aether field effects on the magnetic moment of a current loop around an aether BH with the comparison of the magnetic moment of the Schwarzchild BH. It is obtained that the magnetic moment decreases quasilinearly with the increase of the parameter c_{14}. As it is obtained in ISCO radius, the magnetic moment increase (decrease) when c_{13} take positive (negative).

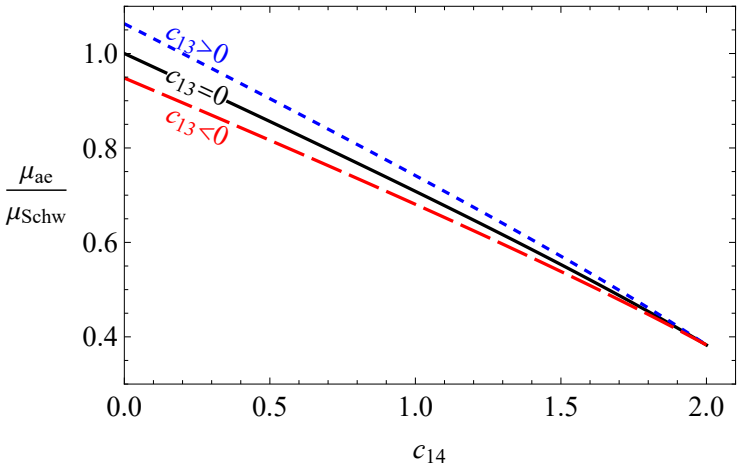

Figure 3. Magnetic moment of current loop around aether BHs as a function of the aether parameter.

Now, it is possible to get non-zero components of the magnetic field around the aether BH in the interior and exterior regions of the ISCO, where the current loop is located using the expression $B^\alpha = (1/2)\eta^{\alpha\beta\gamma\sigma}F_{\beta\gamma}u_\sigma$, with respect to proper observer, where $u_\sigma = -\sqrt{f(r)}(1,0,0,0)$, in the following form:

$$B^{\hat{r}}_{in} = B_{in}\left(1+\alpha\frac{M^2}{r^2}\right)\cos\theta\,, \tag{38}$$

$$B^{\hat{\theta}}_{in} = B_{in}\sqrt{f(r)}\sin\theta\,, \tag{39}$$

with

$$B_{in} = -\frac{3}{4}\frac{\mu}{(1+\alpha)^{\frac{3}{2}}M^3}\left[\frac{2\sqrt{1+\alpha})M(r_0+M)}{r_0^2+\alpha M^2} + \ln\left(1-\frac{2M\sqrt{1+\alpha}}{r_0-M(1-\sqrt{1+\alpha})}\right)\right], \tag{40}$$

and

$$B^{\hat{r}}_{ex} = -\frac{3}{4}\frac{\mu\cos\theta}{(1+\alpha)^{\frac{3}{2}}M^3}\Big[\frac{2\sqrt{1+\alpha})M}{r}\left(1+\frac{M}{r}\right) + \left(1+\alpha\frac{M^2}{r^2}\right)\ln\left(1-\frac{2M\sqrt{1+\alpha}}{r-M(1-\sqrt{1+\alpha})}\right)\Big] \quad (41)$$

$$B^{\hat{\theta}}_{ex} = \frac{3}{4}\frac{\mu\sin\theta}{(1+\alpha)^{\frac{3}{2}}M^3}\Big[\frac{2\sqrt{1+\alpha})M}{r\sqrt{f(r)}}\left(1-\frac{M}{r}\right) + \sqrt{f(r)}\ln\left(1-\frac{2M\sqrt{1+\alpha}}{r-M(1-\sqrt{1+\alpha})}\right)\Big], \quad (42)$$

respectively.

Now we analyse the effects of the aether field on the magnetic field around the BHs.

In Figure 4 we provide an analysis of aether field effects on the radial and angular components of the magnetic field generated by a current loop around a static aether BH, for different values of c_{13} and fixed value of $c_{14} = 0.5$. One can see from the figure that with the presence of c_{14}, the magnetic field decreases, due to the decrease of the magnetic dipole moment (see Figure 3). Moreover, the magnetic field increases (decreases) sufficiently when c_{13} is positive (negative).

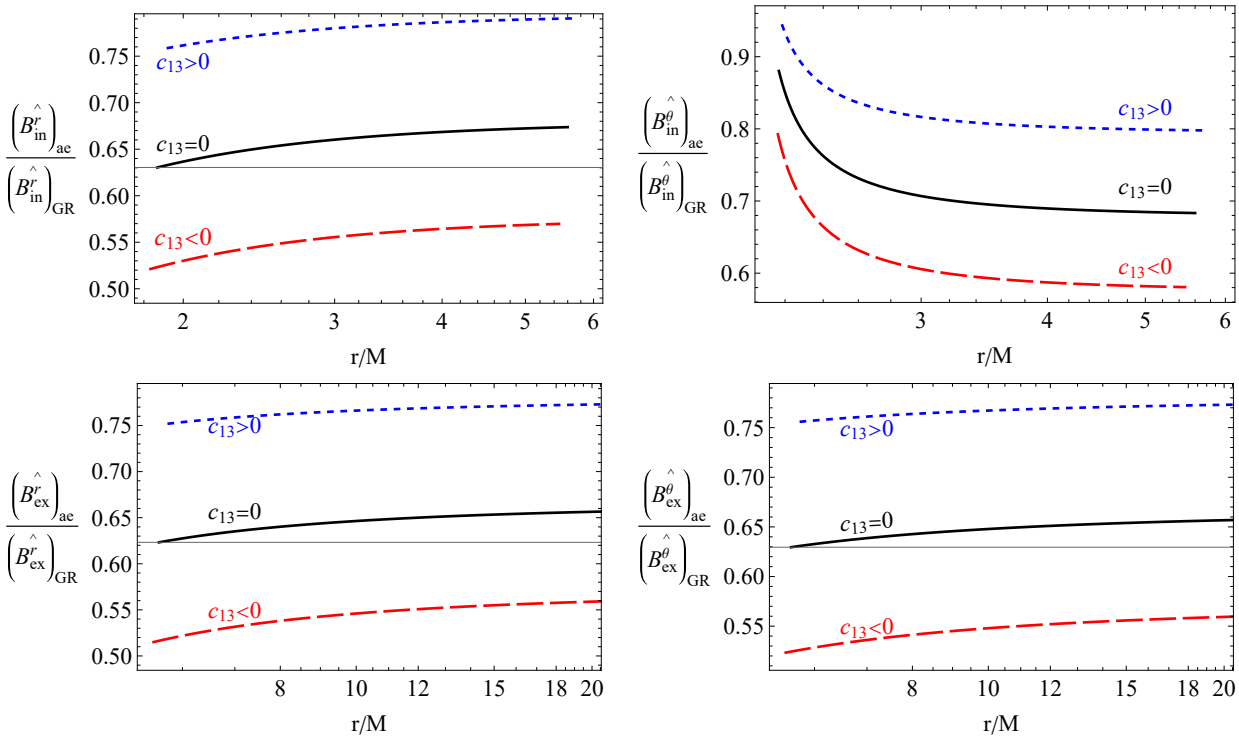

Figure 4. Radial profiles of magnetic field vector's radial (**left column**) and angular (**right column**) components in the interior (**top row**) and exterior (**bottom row**) regions of the current loop around the aether BHs. Here, the parameter c_{14} is chosen as $c_{14} = 0.5$.

5. Conclusions

In this work, we have studied the analytical solutions of the field and motion differential equations in the background of an aether BH, where symmetries of the spacetime are provided. In particular, we have also studied the structure of the magnetic field generated by a current loop around static BHs in Einstein's aether gravity, assuming the electric current loop is located at/close to ISCO. To do this, we first investigated the circular motion of test particles, deriving effective potential for the radial motion of the particles around a

special class of static aether BH. We have tested the effects of the aether field on the position of ISCO of the test particles.

Then, we have derived Maxwell's equations for electromagnetic four-potentials generated by the stationary current loop around the BH. Axial symmetry and stationary properties of the spacetime do allow finding exact analytical equations in the given gravitational background. The exact solutions of Maxwell's equations for magnetic fields have been found, using the spacetime symmetries in the interior and exterior regions of the current loop for the proper observer. In order to solve the derived second-order ordinary differential equation for the vector potential of the electromagnetic field, we have used the spacetime symmetries to separate the variables.

We have also studied the effects of the aether field on the dipole magnetic moment of the current loop and magnetic fields in both regions, and it is shown that the magnetic fields decrease with the increase of the aether parameter c_{14}. Moreover, our analyses have shown that the aether field causes decreasing magnetic field both inside and outside the current loop due to the shift of the ISCO position where the loop is located.

The obtained results can be applied to constrain the Einstein-aether theory through astronomical observations of magnetic fields around astrophysical BHs.

Author Contributions: Conceptualization, J.R. and B.A.; methodology, J.R.; software, J.R.; validation, B.A., J.R. and E.K.; formal analysis, J.R. and E.K.; investigation, B.A. and J.R. All authors have read and agreed to the published version of the manuscript.

Funding: Ministry of Innovative Development of the Republic of Uzbekistan: F-FA-2021-432, F-FA-2021-510, and MRB-2021-527.

Institutional Review Board Statement: Not applicable.

Informed Consent Statement: Not applicable.

Data Availability Statement: Not applicable.

Acknowledgments: This research is supported by Grants F-FA-2021-432, F-FA-2021-510, and MRB-2021-527 of the Uzbekistan Ministry for Innovative Development. J.R. also thanks to the ERASMUS+ project 608715-EPP-1-2019-1-UZ-EPPKA2-JP (SPACECOM).

Conflicts of Interest: The authors declare no conflict of interest.

References

1. Jacobson, T. Einstein-aether gravity: A status report. *arXiv* **2008**, arXiv:0801.1547.
2. Haghani, Z.; Harko, T.; Sepangi, H.R.; Shahidi, S. The scalar Einstein-aether theory. *arXiv* **2014**, arXiv:1404.7689.
3. Jacobson, T.; Mattingly, D. Gravity with a dynamical preferred frame. *Phys. Rev. D* **2001**, *64*, 024028. [CrossRef]
4. Li, B.; Mota, D.F.; Barrow, J.D. Detecting a Lorentz-violating field in cosmology. *Phys. Rev. D* **2008**, *77*, 024032. [CrossRef]
5. Battye, R.A.; Pace, F.; Trinh, D. Cosmological perturbation theory in generalized Einstein-Aether models. *Phys. Rev. D* **2017**, *96*, 064041. [CrossRef]
6. Meiers, M.; Saravani, M.; Afshordi, N. Cosmic censorship in Lorentz-violating theories of gravity. *Phys. Rev. D* **2016**, *93*, 104008. [CrossRef]
7. Lin, K.; Ho, F.H.; Qian, W.L. Charged Einstein-æther black holes in n-dimensional spacetime. *Int. J. Mod. Phys. D* **2019**, *28*, 1950049–1950308. [CrossRef]
8. Azreg-Aïnou, M.; Chen, Z.; Deng, B.; Jamil, M.; Zhu, T.; Wu, Q.; Lim, Y.K. Orbital mechanics for, and QPOs' resonances in, black holes of Einstein-Æther theory. *arXiv* **2020**, arXiv:2004.02602.
9. Zhang, C.; Zhao, X.; Wang, A.; Wang, B.; Yagi, K.; Yunes, N.; Zhao, W.; Zhu, T. Gravitational waves from the quasicircular inspiral of compact binaries in Einstein-aether theory. *Phys. Rev. D* **2020**, *101*, 044002. [CrossRef]
10. Oost, J.; Mukohyama, S.; Wang, A. Constraints on Einstein-aether theory after GW170817. *Phys. Rev. D* **2018**, *97*, 124023. [CrossRef]
11. Zhu, T.; Wu, Q.; Jamil, M.; Jusufi, K. Shadows and deflection angle of charged and slowly rotating black holes in Einstein-Æther theory. *Phys. Rev. D* **2019**, *100*, 044055. [CrossRef]
12. Eling, C.; Jacobson, T.; Miller, M.C. Neutron stars in Einstein-aether theory. *Phys. Rev. D* **2007**, *76*, 042003. [CrossRef]
13. Eling, C.; Jacobson, T. Spherical solutions in Einstein-aether theory: Static aether and stars. *Class. Quantum Gravity* **2006**, *23*, 5625–5642. [CrossRef]
14. Wald, R.M. Black hole in a uniform magnetic field. *Phys. Rev. D.* **1974**, *10*, 1680–1685. [CrossRef]

15. Petterson, J.A. Magnetic field of a current loop around a Schwarzschild black hole. *Phys. Rev. D* **1974**, *10*, 3166–3170. [CrossRef]
16. Petterson, J.A. Stationary axisymmetric electromagnetic fields around a rotating black hole. *Phys. Rev. D* **1975**, *12*, 2218–2225. [CrossRef]
17. Turimov, B. Electromagnetic fields in vicinity of tidal charged static black hole. *Int. J. Mod. Phys. D* **2018**, *27*, 1850092. [CrossRef]
18. Deutsch, A.J. The electromagnetic field of an idealized star in rigid rotation in vacuo. *Ann. d'Astrophysique* **1955**, *18*, 1.
19. Rezzolla, L.; Ahmedov, B.J.; Miller, J.C. General relativistic electromagnetic fields of a slowly rotating magnetized neutron star-I. Formulation of the equations. *Mon. Not. R. Astron. Soc.* **2001**, *322*, 723–740. [CrossRef]
20. Ahmedov, B.J.; Fattoyev, F.J. Magnetic fields of spherical compact stars in a braneworld. *Phys. Rev. D* **2008**, *78*, 047501. [CrossRef]
21. Turimov, B.V.; Ahmedov, B.J.; Hakimov, A.A. Stationary electromagnetic fields of slowly rotating relativistic magnetized star in the braneworld. *Phys. Rev. D* **2017**, *96*, 104001. [CrossRef]
22. Turimov, B.; Ahmedov, B.; Abdujabbarov, A.; Bambi, C. Electromagnetic fields of slowly rotating magnetized compact stars in conformal gravity. *Phys. Rev. D* **2018**, *97*, 124005. [CrossRef]
23. Rayimbaev, J.; Turimov, B.; Marcos, F.; Palvanov, S.; Rakhmatov, A. Particle acceleration and electromagnetic field of deformed neutron stars. *Mod. Phys. Lett. A* **2020**, *35*, 2050056. [CrossRef]
24. Bokhari, A.H.; Rayimbaev, J.; Ahmedov, B. Radio loudness and spindown of pulsars in Einstein-aether gravity. *Phys. Dark Universe* **2021**, *34*, 100901. [CrossRef]
25. Piotrovich, M.Y.; Silant'ev, N.A.; Gnedin, Y.N.; Natsvlishvili, T.M. Magnetic Fields of Black Holes and the Variability Plane. *arXiv* **2010**, arXiv:1002.4948.
26. Event Horizon Telescope Collaboration; Akiyama, K.; Algaba, J.C.; Alberdi, A.; Alef, W.; Anantua, R.; Asada, K.; Azulay, R.; Baczko, A.K.; Ball, D.; et al. First M87 Event Horizon Telescope Results. VIII. Magnetic Field Structure near The Event Horizon. *Astrophys. J. Lett.* **2021**, *910*, L13. [CrossRef]
27. Eatough, R.P.; Falcke, H.; Karuppusamy, R.; Lee, K.J.; Champion, D.J.; Keane, E.F.; Desvignes, G.; Schnitzeler, D.H.F.M.; Spitler, L.G.; Kramer, M.; et al. A strong magnetic field around the supermassive black hole at the centre of the Galaxy. *Nature* **2013**, *501*, 391–394. [CrossRef]
28. Foster, B.Z. Radiation damping in Einstein-aether theory. *Phys. Rev. D* **2006**, *73*, 104012. [CrossRef]
29. Garfinkle, D.; Eling, C.; Jacobson, T. Numerical simulations of gravitational collapse in Einstein-aether theory. *Phys. Rev. D* **2007**, *76*, 024003. [CrossRef]
30. Ding, C.; Wang, A.; Wang, X. Charged Einstein-aether black holes and Smarr formula. *Phys. Rev. D* **2015**, *92*, 084055. [CrossRef]
31. Stuchlík, Z.; Kološ, M.; Kovář, J.; Slaný, P.; Tursunov, A. Influence of Cosmic Repulsion and Magnetic Fields on Accretion Disks Rotating around Kerr Black Holes. *Universe* **2020**, *6*, 26. [CrossRef]
32. Stuchlík, Z.; Kološ, M.; Tursunov, A. Penrose Process: Its Variants and Astrophysical Applications. *Universe* **2021**, *7*, 416. [CrossRef]